J|A|C|S ARTICLES

Published on Web 12/08/2009

Tailored Electrochemical Synthesis of 2D-Hexagonal, Lamellar, and Cage-Type Mesostructured Pt Thin Films with Extralarge Periodicity

Azusa Takai,[†] Yusuke Yamauchi,*[,†,‡,§] and Kazuyuki Kuroda*[,†]

Faculty of Science & Engineering, Waseda University, Ohkubo 3-4-1, Shinjuku, Tokyo 169-8555, Japan, World Premier International (WPI) Research Center for Materials Nanoarchitectonics (MANA), National Institute for Materials Science (NIMS), 1-1 Namiki, Tsukuba, Ibaraki 305-0044, Japan, and Precursory Research for Embryonic Science and Technology (PRESTO), Japan Science and Technology Agency (JST), Kawaguchi, Saitama 332-0012, Japan

Received July 27, 2009; E-mail: Yamauchi.Yusuke@nims.go.jp; kuroda@waseda.jp

Abstract: We report the synthesis of mesostructured Pt films with extralarge periodicity from lyotropic liquid crystals consisting of block copolymers (polystyrene-*b*-polyethylene oxide, PS-*b*-PEO) on Au substrates by electrochemical deposition. The Pt films with three types of (two-dimensional (2D)-hexagonal, lamellar, and cage-type) mesostructures are successfully synthesized by controlling the compositional ratio between block copolymers and Pt species in precursor solutions. The mesostructured Pt films have high electrochemically active surface areas. The bumpy mesopore surfaces, which reflect the mesopore walls consisting of connected nanoparticles, greatly contribute to the enhancement of the surface areas. The mesopore walls have single crystal domains over 400 nm^2 region proved by the lattice fringes of Pt extending over several nanoparticles.

1. Introduction

Since the first reports,[1,2] ordered mesoporous materials with various framework compositions have been synthesized through self-organization of surfactants.[3−9] Among them, mesoporous metals hold promise for a wide range of potential applications, such as metal catalysts and electrodes, owing to their metallic frameworks. Mesoporous metals have been synthesized by the reduction of metal ions dissolved in lyotropic liquid crystals (LLC) consisting of highly concentrated surfactants.[10,11] Successful control over the metallic compositions and morphologies is a key factor for the enhancement of their functionalities and the generation of the properties of new materials. To date, mesoporous alloys with tunable compositions have been designed through the coreduction of different metal species.[12−15] In addition, the collaboration of both LLC and hard templates, such as porous anodic alumina, has led to the versatile control of the morphologies (e.g., nanorods,[16] nanotubes[17]).

Despite such progress, the versatile controls of pore size and pore geometries remain as major challenges. Most of the mesoporous metals reported previously have been limited to only a two-dimensional (2D) hexagonal mesostructure with mesopores less than 3 nm in diameter.[10−17] Such a limit of mesopore size seriously devalues the advantages of mesoporous metals because the small mesopores do not work effectively in reaction to large-size molecules.[18] It was recently shown that block copolymer self-assembly provided access to large mesoporous structures, and mesoporous Pt *powders* were obtained.[19,20] However, such powdery morphology is of limited relevance for electrochemical or sensor devices in which the mesoporous metals are required as thin *films*. Furthermore, the design of various mesostructures in mesoporous metal films is also demanded because the characteristic functions vary depending

[†] Waseda University.
[‡] WPI Center for MANA, NIMS.
[§] PRESTO, JST.

(1) Yanagisawa, T.; Shimizu, T.; Kuroda, K.; Kato, C. *Bull. Chem. Soc. Jpn.* **1990**, *63*, 988.
(2) Kresge, C. T.; Leonowicz, M. E.; Roth, W. J.; Vartuli, J. C.; Beck, J. S. *Nature* **1992**, *359*, 710.
(3) Yang, P.; Zhao, D.; Margolese, D. I.; Chmelka, B. F.; Stucky, G. D. *Nature* **1998**, *396*, 152.
(4) Wan, Y.; Zhao, D. *Chem. Rev.* **2007**, *107*, 2821.
(5) Schüth, F. *Chem. Mater.* **2001**, *13*, 3184.
(6) Schüth, F.; Schmidt, W. *Adv. Mater.* **2002**, *14*, 629.
(7) Inagaki, S.; Guan, S.; Ohsuna, T.; Terasaki, O. *Nature* **2002**, *416*, 304.
(8) Meng, Y.; Gu, D.; Zhang, F.; Shi, Y.; Yang, H.; Li, Z.; Yu, C.; Tu, B.; Zhao, D. *Angew. Chem., Int. Ed.* **2005**, *44*, 7053.
(9) Kondo, J. N.; Domen, K. *Chem. Mater.* **2008**, *20*, 835.
(10) Attard, G. S.; Bartlett, P. N.; Coleman, N. R. B.; Elliott, J. M.; Owen, J. R.; Wang, J. H. *Science* **1997**, *278*, 838.
(11) Attard, G. S.; Göltner, C. G.; Corker, J. M.; Henke, S.; Templer, R. H. *Angew. Chem., Int. Ed.* **1997**, *36*, 1315.
(12) Yamauchi, Y.; Kuroda, K. *Chem. Asian J.* **2008**, *3*, 664.
(13) Attard, G. S.; Leclerc, S. A. A.; Maniguet, S.; Russell, A. E.; Nandhakumar, I.; Bartlett, P. N. *Chem. Mater.* **2001**, *13*, 1444.
(14) Jiang, J.; Kucernak, A. *Chem. Mater.* **2004**, *16*, 1362.
(15) Yamauchi, Y.; Ohsuna, T.; Kuroda, K. *Chem. Mater.* **2007**, *19*, 1335.
(16) Yamauchi, Y.; Takai, A.; Nagaura, T.; Inoue, S.; Kuroda, K. *J. Am. Chem. Soc.* **2008**, *130*, 5426.
(17) Takai, A.; Yamauchi, Y.; Kuroda, K. *Chem. Commun.* **2008**, 4171.
(18) For a silica case)Sun, J.; Zhang, H.; Tian, R.; Ma, D.; Bao, X.; Su, D. S.; Zou, H. *Chem. Commun.* **2006**, 1322.
(19) Warren, S. C.; Messina, L. C.; Slaughter, L. S.; Kamperman, M.; Zhou, Q.; Gruner, S. M.; DiSalvo, F. J.; Wiesner, U. *Science* **2008**, *320*, 1748.
(20) Yamauchi, Y.; Sugiyama, A.; Morimoto, R.; Takai, A.; Kuroda, K. *Angew. Chem., Int. Ed.* **2008**, *47*, 5371.

 10.1021/ja9062844

on the mesostructures. The 2D-hexagonal mesostructure has higher accessibility than other mesostructures due to its straight tubular channels.[21] Cage-type mesostructured films with windows between mesopores have potential use as host materials of nanoreactors which have only been realized in powdery silica systems.[22]

The replication method by using hard templates, such as mesoporous silica, zeolites, and porous membranes, has also been introduced as another way for synthesis of mesostructured metals.[23−30] The mesostructures of final products reflect those of original hard templates. The final products possess inverse mesostructures of their templates (i.e., spherical (zero-dimensional, 0D) or wire (1D) arrays). This process is powerful for preparing mesoporous materials with various compositions which are more difficult to be synthesized by conventional processes. These ordered mesoporous materials have been reviewed in several papers.[23−25] However, this procedure involves multisteps and harsh (e.g., alkaline condition) treatments to remove templates. In contrast, the soft-templating method using a LLC system has several advantages; one-step synthesis, mild experimental conditions for the removal of LLC, versatile controls of morphologies and compositions as mentioned above.[12−17] Therefore, we have focused on the LLC systems for synthesis of mesoporous metals.

In this paper, we propose the synthesis of 2D-hexagonal, lamellar, and cage-type mesostructured Pt thin films with extralarge periodicity electrodeposited from block copolymer-based LLC formed on Au substrates (Figure 1). By changing the compositional ratio between block copolymer and Pt species of a precursor solution, the mesostructures in the metal films can be finely controlled from cage-type to 2D-hexagonal and lamellar mesostructures.

2. Experimental Section

2.1. Materials. Hydrogen hexachloroplatinate(IV) hydrate ($H_2PtCl_6 \cdot 6H_2O$, Kanto Kagaku Co.) was used as a Pt source. Tetrahydrofuran (THF, Wako Chemical Co.) was used for both the dilution of the precursor solution and the removal of templates. Poly(styrene-*b*-ethylene oxide) block copolymer (PS_{3800}-*b*-PEO_{4800}) was purchased by Polymer Source, Inc.

2.2. Synthesis of 2D-Hexagonal, Lamellar, and Cage-Type Mesostructured Pt Thin Films. All of the experiments were carried out at the room temperature (about 25 °C). For preparing precursor solutions, PS-*b*-PEO (0.25 g) was dissolved in THF (12.5 g) and stirred for 1 h. After adding 50 wt % aqueous solution of $H_2PtCl_6 \cdot 6H_2O$ (0.10−0.80 mL), the solutions were stirred for 1 h. The added amounts of Pt aqueous solution was changed depending on the mesostructures: 0.10 mL for lamellar, 0.30−0.50 mL for 2D-hexagonal, and 0.80−1.50 mL for cage-type mesostructures, respectively. After the resultant precursor solutions were drop-coated onto a Au-coated Si substrate, LLC films were formed immediately through solvent evaporation of THF. Pt species in the LLC films were electrodeposited at a constant potential (−0.10 V vs Ag/AgCl) by using a potentiostat/galvanostat HA-151 (Hokuto Denko Corp.). The experimental procedures are described in Scheme 1. After electrodeposition, the block copolymer and the undeposited Pt species were removed with THF and water. From the XPS (X-ray photoelectron spectroscopy) spectrum of the samples after washing, the peaks assigned to chloride ions of H_2PtCl_6 were not observed at around 198 eV (Figure S1). Also, any undeposited Pt species such as Pt^{4+} were not observed, though intense two peaks assigned to Pt^0 $4f_{7/2}$ and Pt^0 $4f_{5/2}$ were observed at 71.0 and 74.0 eV, respectively (Figure S2).[31] Furthermore, in the IR (infrared spectroscopy) spectra of the samples after washing, any peaks derived from aromatic rings of the block copolymers were not observed (not shown). On the basis of these results, it can be explained that the block copolymers and undeposited Pt species were successfully removed by washing with THF and water.

2.3. Characterizations. Small angle X-ray scattering (SAXS) patterns were measured using a Rigaku Nano viewer with Cu Kα

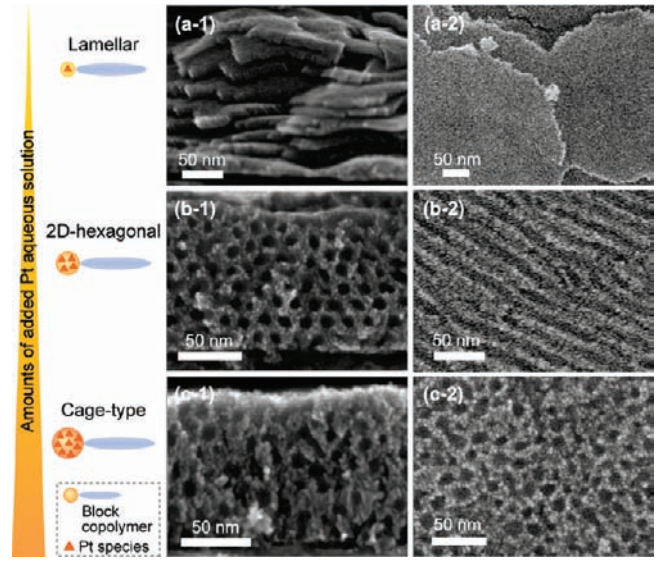

Figure 1. Overview of this study. High-resolution SEM images of (a) lamellar, (b) 2D-hexagonal, and (c) cage-type mesostructured films. (a-1, b-1, and c-1) Cross-sectional images and (a-2, b-2, and c-2) top-surface images.

Scheme 1. Schematic View of a Preparative Procedure for Mesoporous Pt Films[a]

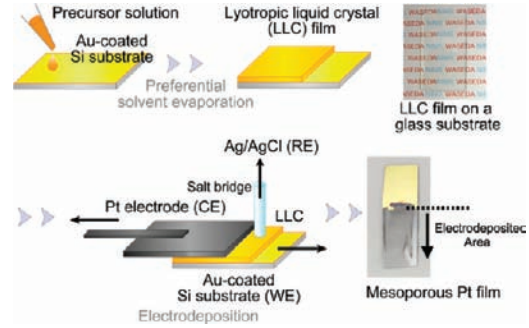

[a] The photographs show a LLC film and a mesoporous Pt film synthesized from precursor solutions including 0.50 mL of a Pt aqueous solution.

(21) Tanaka, H. K. M.; Yamauchi, Y.; Kurihara, T.; Sakka, Y.; Kuroda, K.; Mills, A. P., Jr. *Adv. Mater.* **2008**, *20*, 4728.
(22) Shui, W.; Fan, J.; Yang, P.; Liu, C.; Zhai, J.; Lei, J.; Yan, Y.; Zhao, D.; Chen, X. *Anal. Chem.* **2006**, *78*, 4811.
(23) Lu, A. H.; Schüth, F. *Adv. Mater.* **2006**, *18*, 1793.
(24) Yang, H.; Zhao, D. *J. Mater. Chem.* **2005**, *15*, 1217.
(25) Tiemann, M. *Chem. Mater.* **2008**, *20*, 961.
(26) Yang, C. M.; Lin, H. A.; Zibrowius, B.; Spliethoff, B.; Schüth, F.; Liou, S. C.; Chu, M. W.; Chen, C. H. *Chem. Mater.* **2007**, *19*, 3205.
(27) Fuertes, M. C.; Marchena, M.; Marchi, M. C.; Wolosiuk, A.; Soler-Illia, G. J. A. A. *Small* **2009**, *5*, 272.
(28) Ko, C. H.; Ryoo, R. *Chem. Commun.* **1996**, 2467.
(29) Zhang, X.; Lu, W.; Da, J.; Wang, H.; Zhao, D.; Webley, P. A. *Chem. Commun.* **2009**, 195.
(30) Wan, Y.; Wang, H.; Zhao, Q.; Klingstedt, M.; Terasaki, O.; Zhao, D. *J. Am. Chem. Soc.* **2009**, *131*, 4541.
(31) Wagner, C. D.; Riggs, W. M.; Davis, L. E.; Moulder, J. F. *In Handbook of X-ray Photoelectron Spectroscopy*; Mullemberg, G. E., Ed.; Perkin-Elmer: Eden Prairie, MN, 1978.

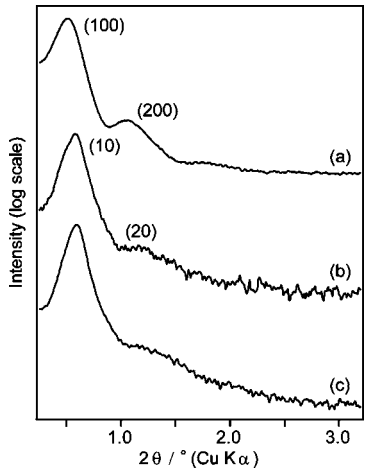

Figure 2. SAXS patterns of (a) lamellar, (b) 2D-hexagonal, and (c) cage-type mesostructured LLC before electrodeposition. Each LLC was prepared from a precursor solution including (a) 0.10, (b) 0.50, and (c) 0.80 mL of a Pt aqueous solution.

radiation (40 kV, 30 mA). SEM images were obtained using a Hitachi HR-SEM S-5500 microscope operating at 30 kV. Samples were observed directly without any coatings. Transmission electron microscopy (TEM) images and electron diffraction (ED) patterns were taken by a JEOL JEM-2010 microscope using an accelerating voltage of 200 kV. For TEM observation, film samples were scratched from the Au substrate and the samples were dispersed in ethanol by ultrasound and mounted on a carbon-coated microgrid (Okenshoji Co.). For the measurement of electrochemically active surface areas, calculated from hydrogen adsorption/desorption on the mesostructured Pt films, cyclic voltammometry (CV) was performed in 1.0 M aqueous H_2SO_4 solution at the potential scan rate of 100 $mV \cdot sec^{-1}$ by a potentiostat/galvanostat HZ-5000 (Hokuto Denko Co.). XPS spectra were taken at room temperature using a JPS-9010TR (JEOL) instrument with a Mg Kα X-ray source. All binding energies were calibrated by referencing C 1s (285.0 eV). FT-IR spectra of the LLC films on Si substrates were obtained by transmission mode with a nominal resolution of 2.0 cm^{-1} on a FT/IR-6100 (JASCO Co.). Liquid-state ^1H NMR (nuclear magnetic resonance) spectra were obtained by using a JEOL ECX-500 spectrometer with resonance frequencies of 500.0 MHz. The sample solutions for the NMR measurement were prepared by dissolving the LLC films in chloroform-*d*. The solutions were put into a 5 mm glass tube. Tetramethylsilane (TMS) was added as an internal reference. Chloroform-*d* was used to obtain lock signals.

3. Results and Discussion

When the amount of the aqueous Pt solution in the precursor solutions ranged from 0.30 to 0.50 mL, mesoporous Pt films with a 2D-hexagonal mesostructure were prepared (Figures 1b, 2b, 3, and 4). The small-angle X-ray scattering (SAXS) patterns of the LLC film before Pt deposition showed obvious peaks with higher-order diffractions (d = 16.5 nm (0.30 mL, not shown) and 15.2 nm (0.50 mL, Figure 2b)).

After the Pt deposition, the obtained films were crack-free and had a uniform thickness of around 100 nm over the entire area (Figures 3 and 4). For the formation of such continuous films, the selection of substrate composition is important. When Pt species in an aqueous Pt solution without block copolymers are electrochemically reduced on Au substrates, the atomic arrangements of the deposited Pt were reflected by those of the Au substrate, as is evidenced by the scanning tunneling microscopic (STM) images.[32] Because the lattice parameters of the deposited Pt are quite similar as those of Au, the

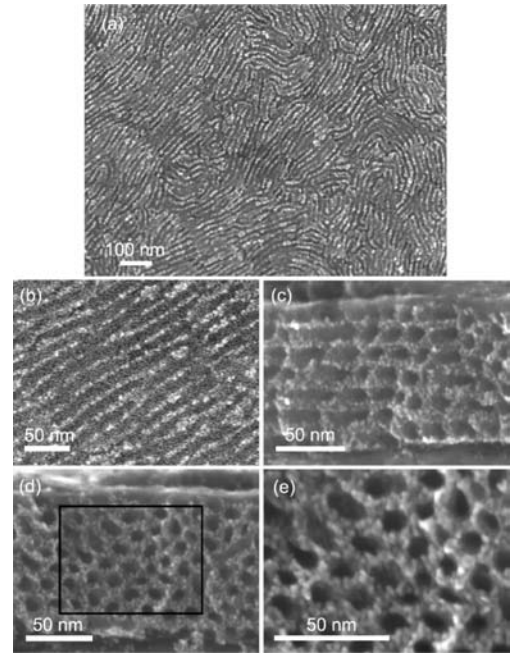

Figure 3. (a and b) Top-surface and (c, d, and e) cross-sectional SEM images of 2D-hexagonal mesostructured Pt films prepared from a precursor solution including 0.50 mL of a Pt aqueous solution. Panel e is a highly magnified image of the square region of panel d. The nanopaticles were assembled to make the frameworks. The cylindrical mesochannels of panel c indicated 2D-hexagonal mesostructures oriented parallel to the substrate, which was also supported from Figure 1b.

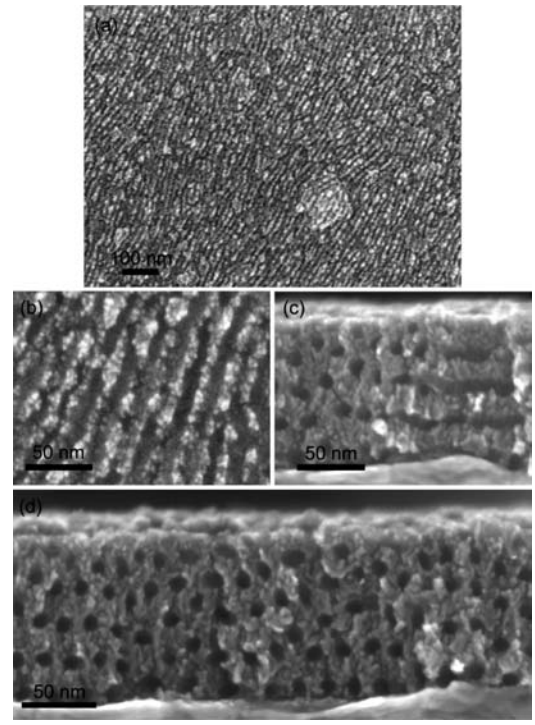

Figure 4. (a and b) Top-surface and (c and d) cross-sectional SEM images of 2D-hexagonal mesostructured Pt films prepared from a precursor solution including 0.30 mL of a Pt aqueous solution.

(32) Uosaki, K.; Ye, S.; Naohara, H.; Oda, Y.; Haba, T.; Kondo, T. *J. Phys. Chem. B* **1997**, *101*, 7566.

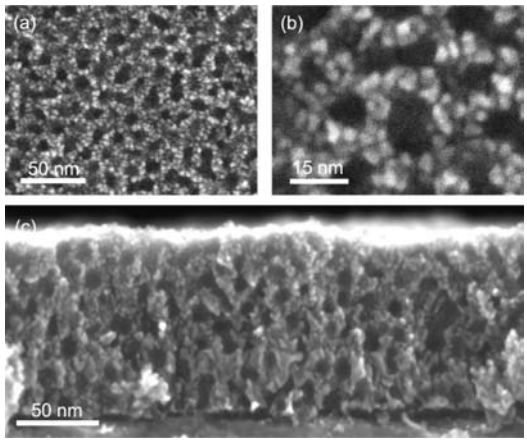

Figure 5. (a and b) Top-surface and (c) cross-sectional SEM images of cage-type mesostructured Pt films prepared from a precursor solution including 0.80 mL of a Pt aqueous solution.

nucleation of Pt easily occurs. Therefore, in the present case, a lot of the Pt nuclei are homogeneously generated on the Au substrate at the initial stage of the Pt deposition. Then, Pt can uniformly grow from the initial Pt nuclei. Therefore, Pt can be continuously deposited over the entire area of the Au substrate. In contrast, when ITO substrates were used instead of Au substrates, granular particles were deposited.[20] The lattice parameters of surface ITO are different from those of Pt. Because of such a mismatch of the parameters, the number of Pt nuclei generated at the initial stage is not sufficient to make a continuous film. The low deposition potential is another necessary factor for continuous crack-free films. The low deposition potential can prevent side reactions such as the evolution of gas at the interface between the LLCs and Au substrates. The evolution of gas has often been the cause of cracks in films. In our electrodeposition conditions, the film growth from the LLC is carried out under mild deposition conditions even though the LLC suppress the diffusion of the metal ions.

From highly magnified images, the top surface of the film showed stripes (Figures 1b−2, 3a,b and 4a,b), which are typical features of mesochannels oriented parallel to the substrate. These stripes were bent rather than aligned in a uniaxial direction. Both the honeycomb arrangements of mesopores and tubular mesochannels (Figures 1b-1, 3c−e, and 4c,d) indicate the formation of 2D-hexagonal mesostructure.

Other mesostructured films, such as cage-type and lamellar structures, were synthesized on substrates by changing the amount of the aqueous Pt solution in the precursor solutions (Figure 1a,c). When the amount of the Pt solution was increased to 0.80 mL, the cage-type of Pt mesostructure was obtained (Figure 5). The aqueous Pt species were strongly interacted with EO groups in LLC, and a stable conformation was formed.[33] With the increase of the Pt species, the size of hydrophilic groups was relatively larger than that of the hydrophobic groups, and the curvature of the block copolymer assemblies was larger, being transformed to a cage-type mesostructure. The SAXS measurement of the LLC film before Pt deposition showed an obvious peak (d = 14.7 nm), and its higher-order diffractions became unclear (Figure 2c). After the deposition, open mesopores of around 10 nm in diameter were observed from the top surface of the film. (Figure 5a,b) The repeat distance was around

(33) Çelik, Ö.; Dag, Ö. *Angew. Chem., Int. Ed.* **2001**, *40*, 3800.

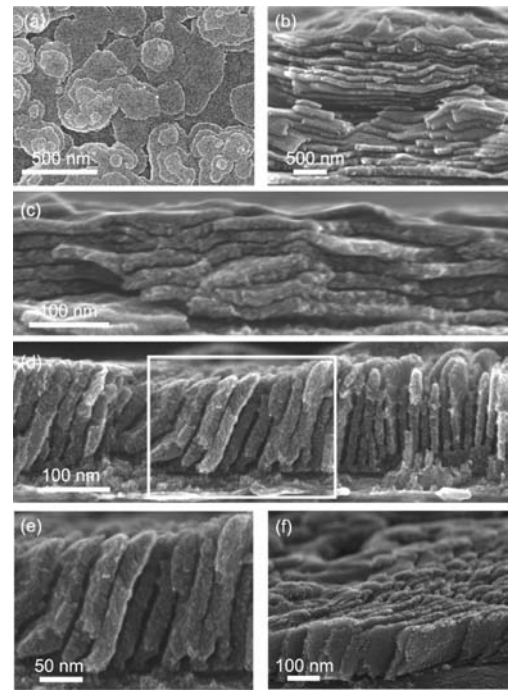

Figure 6. (a) Top-surface and (b−f) cross-sectional SEM images of lamellar mesostructured Pt films prepared from a precursor solution including 0.10 mL of a Pt aqueous solution. Panel e is a highly magnified image of the square region of panel d.

15 nm, which was consistent with the SAXS data (Figure 2c). From the cross-sectional SEM images, the spherical mesopores were observed in the inner part of the film, indicating that mesopores were present all over the film (Figure 5c) and that they were packed randomly and interconnected with each other.

On the other hand, LLC films with a lamellar mesostructure were formed by adding a smaller amount (0.10 mL) of the Pt aqueous solution (Figure 1a). The SAXS pattern of LLC films showed intense peaks (d = 17.3 nm) (Figure 2a). After the Pt deposition, stacked layers with a parallel orientation to the substrates were mainly observed over a large area (Figures 1a and 6a−c). In very small domains, layers were accidentally oriented perpendicularly to the substrate and/or tilted (Figures 6d−f). The standing layers ran across the film. The alignment transition in a perpendicular direction was thought to occur during Pt deposition. This phenomenon would be due to the gradual increase of the Pt ion concentration locally near the interface between the LLC film and the Au substrate. Although the mechanism for the local perpendicular orientation is unclear, a previous system of PS-*b*-PMMA with large amounts of Li^+ and Cl^- ions shows a similar situation,[34] in which both of the ions are present at the interface between the polymer and the substrate,[35] inducing the transition of the orientation of lamellar mesophase possibly due to the change of the interfacial interaction.

In the 2D-hexagonal systems, however, a perpendicular orientation was not observed. It could be due to the difference in the mobility of LLC. The 2D-hexagonal LLC with higher concentrated Pt species is more stable and rigid because more Pt ions interacted with EO groups.[31] Therefore, the 2D-

(34) Wang, J. Y.; Chen, W.; Sievert, J. D.; Russell, T. P. *Langmuir* **2008**, *24*, 3545.
(35) Wang, J. Y.; Xu, T.; Leiston-Belanger, J. M.; Gupta, S.; Russell, T. P. *Phys. Rev. Lett.* **2006**, *96*, 128301.

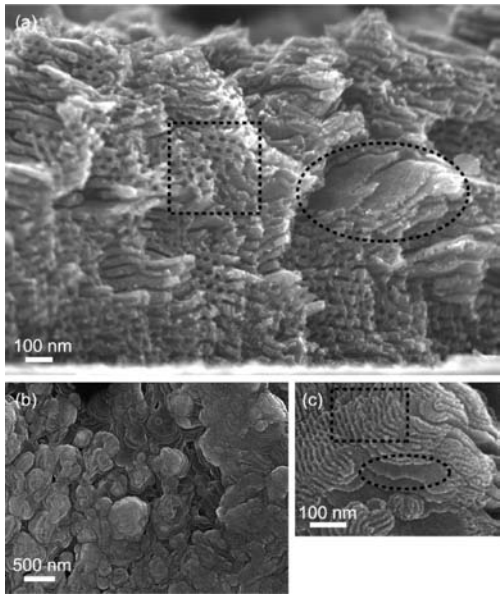

Figure 7. (a) Cross-sectional and (b and c) top-surface SEM images of mesostructured Pt films with mixed phases of both 2D-hexagonal and lamellar mesostructures, prepared from a precursor solution including 0.20 mL of a Pt aqueous solution. Dotted circular and square regions are typical images of lamellar and 2D-hexagonal structure, respectively.

hexagonal and cage-type LLC mesostructures can be strictly fixed during the Pt deposition, while the lamellar LLC is assumed to move by the change in the concentration of Pt ions during the deposition. In fact, the thicknesses of the layers of the lamellar Pt film varied from 15 to 50 nm depending on the location; that is, the observed periodicity largely changed from that of the original LLC film (Figure 6b−e).

Furthermore, the lamellar Pt film showed a stacked discontinuous plate-like morphology, which is in contrast to the continuous films with 2D-hexagonal and cage-type mesostructures (Figures 1a-2 and 6a). The difference is due to the Pt deposition behavior in LLC. In the 2D-hexagonal and cage-type LLC, hydrophilic domains with the Pt species are continuously present over the entire films. Therefore, Pt species can be uniformly attracted around Pt nuclei, which are generated onto Au substrates at a very early stage of electrodeposition, making continuous films with uniform thickness. It is possible to finely control the film thickness by changing the deposition time. In lamellar LLC, however, Pt species were preferably moved along the parallel direction to the substrate because the diffusion of the Pt species was limited due to the sheetlike hydrophilic domains.

Mixed phases (i.e., lamellar and 2D-hexagonal mesostructures, 2D-hexagonal, and cage-type mesostructures) were deposited by adding an intermediate amount of the Pt solution. When 0.20 mL of the Pt solution was added, cross-sectional images indicated the presence of both layered and honeycomb mesostructures at the same time, which is the typical structure of lamellar and 2D-hexagonal mesostructures, respectively (Figure 7). On the other hand, when the added amount was 0.70 mL, both curved tubular mesochannels (Figure 8a) and closely packed mesocages (Figure 8b) were observed. The 2D-hexagonal domain was much smaller than those of the 2D-hexagonal films (Figures 3a and 4a). The formation of the mixed phase is strong evidence that the phase transition occurred gradually depending on the amount of the Pt species in the LLC.

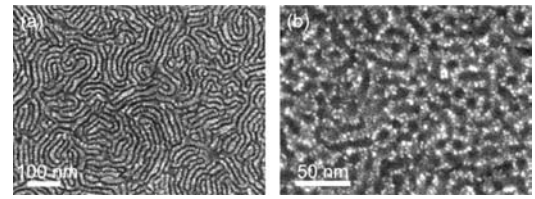

Figure 8. Top-surface SEM images of mesostructured Pt films with mixed phases of 2D-hexagonal and cage-type mesostructures, prepared from a precursor solution including 0.70 mL of a Pt aqueous solution.

The mesostructural control can generally be discussed by packing parameters of block copolymers with inorganic units.[36,37] The similar phase transition have been studied on LLC mesostructures of a ternary (H_2PtCl_6 + water + $C_{16}EO_8$ as a surfactant) system.[38] When the concentration of the Pt species in water was fixed, the LLC mesostructures were changed from lamellar to bicontinuous cubic ($Ia\bar{3}d$), 2D-hexagonal, and finally micelle cubic with the increase of the weight ratios of the aqueous Pt solutions to the surfactants. Because the EO groups of the surfactants can accommodate metal aqua complexes through hydrogen bonds,[33] the apparent size of the complex EO group with metal ions becomes bigger as the ratio of the Pt solutions is increased. This phenomenon should be applied to our present study using PS-*b*-PEO with the same hydrophilic compositions (EO groups). In the IR spectrum of the LLC film prepared from a precursor solution including 0.50 mL of Pt aqueous solution, an absorption band around 1079 cm^{-1} assigned to the C−O stretching vibration of PEO groups was slightly shifted to lower energy (Supporting Information, Figure S3),[33] indicating the same phenomenon on the formation of hydrogen bonding between Pt aqua complexes and PEO groups. Therefore, the increase in the volume of hydrophilic head groups to hydrophobic tail groups induces the transitions from lamellar to 2D hexagonal, and further transition to cage-type mesostructure.

The phase transitions of the mesostructured Pt system in the present study are different from those of mesostructured silica systems. Mesostructured silica films prepared by the EISA (evaporation-induced self-assembly) method are synthesized from $PEO_{20}-PPO_{70}-PEO_{20}$ triblock copolymer (P123) and tetraethoxysilane (TEOS). The number of Si atoms to one EO unit is, as a typical example, 0.95 for lamellar, 2.7 for 2D-hexagonal, and 4.3 cage-type ($Im\bar{3}m$) mesostructures, respectively.[36] In the present case, it is necessary to add smaller amounts of Pt species and to change the ratio of Pt/EO unit in a much larger scale. The number of Pt species to one EO unit was 0.030 for lamellar, 0.092−0.15 for 2D-hexagonal, and 0.24 for cage-type mesostructures. The difference may be due to the difference of the interaction strength between the inorganic species and the EO units. In both systems, inorganic species and EO units form hydrogen bonding. Unlike silica cases, the Pt complexes do not form oligomers but are present independently as an aqua complex.[33] Therefore, the Pt aqua complexes are expected to be more effectively interacted with the EO units. Even small amounts of Pt complexes can densely entangle lots of EO units in the LLC, forming a stable conformation. When

(36) Alberius, P. C. A.; Frindell, K. L.; Hayward, R. C.; Kramer, E. J.; Stucky, G. D.; Chmelka, B. F. *Chem. Mater.* **2002**, *14*, 3284.
(37) Huo, Q.; Leon, R.; Petroff, P. M.; Stucky, G. D. *Science* **1995**, *268*, 1324.
(38) Attard, G. S.; Bartlett, P. N.; Coleman, N. R. B.; Elliott, J. M.; Owen, J. R. *Langmuir* **1998**, *14*, 7340.

$C_{16}EO_8$ is used for the synthesis of mesoporous Pt, the number of Pt species to one EO unit is 0.10 for 2D-hexagonal mesostructures,[38] which corresponds to the present PS-*b*-PEO system. These finding should be important for the synthesis of mesostructured Pt by using soft-templates.

It should be noted that our synthetic procedure of mesoporous metals through solvent evaporation is completely different from the EISA method for the synthesis of mesoporous silica and other metal oxides films. In the case of the EISA system, as the organic solvent is gradually evaporated, the inorganic frameworks (such as silica and metal oxides) are simultaneously formed through sol−gel reaction of inorganic species.[2−9,36,37] Therefore, the obtained mesostructures are strongly dependent on the temperatures and times of the solvent evaporation. Disordered structures or mixed mesophases have often been observed. The fine control of the evaporation process is quite important for making highly ordered mesoporous films.[39−41] In our case, however, these factors on the solvent evaporation (temperatures and times of solvent evaporation, and both kind and amount of organic solvents) do not influence the LLC mesostructure at all. Our precursor solutions for the LLC formation consist of amphiphilic molecules (as templates), inorganic species (metal salts), water, and volatile organic solvents.[12,42] The LLC are gradually formed through the evaporation of the organic solvents. Unlike the EISA system, metal species are not reacted (including reduction) during the solvent evaporation. The LLC mesostructures after the solvent evaporation are determined by the compositional ratio of metal solutions and block copolymers. The LLC mesostructures can be directly predicted by a certain phase diagram of ternary compositions (surfactant, water, and metal species) independent of the amount of organic solvent. After the LLC formation on substrates, metals are deposited in the presence of LLC. The final mesostructures basically reflect those of the LLC.

In the present system, THF was used as the volatile organic solvent to dissolve the block copolymers. The SAXS patterns of the LLC mesostructures after THF evaporation did not change at all, irrespective of the amount of THF solvent. After the LLC films were formed on the substrates, THF was completely evaporated, as was confirmed by the NMR spectrum (Supporting Information, Figure S4). Even when the evaporation speed of THF was accelerated under higher temperatures, the mesostructures of the LLC films prepared from the same precursor solutions were identical. Consequently, our process is quite different from the conventional EISA method. To distinguish the difference between the conventional EISA method and ours, we named our process as "evaporation-mediated direct templating (EDIT)".[12] Recently, this EDIT procedure has been applied to other metal systems by different research groups for the synthesis of mesoporous metals and semiconductors.[43,44]

It should be noted that the mesopore walls had bumpy surfaces composed of connected nanoparticles (Figures 3e and 5c), and the fact of the formation of bumpy surfaces is a unique characteristic of the metal deposition in LLC. It has been reported that metal nanoparticles are assembled to make thin films.[45] Such films are of interest for their potential applications owing to their high surface areas, and the random micropores are derived from the voids among the assembled nanoparticles. Our mesoporous Pt films possess ordered mesospaces, and the framework is composed of connected nanoparticles, which should increase the electrochemically active surface area and improve mass diffusion efficiency of guest molecules. A highly magnified TEM observation of the 2D-hexagonal mesoporous Pt film revealed that the Pt atomic crystallinity is coherently extended across at least more than 10 nanoparticles (Figure 9). The single crystal domain was over 400 nm^2 regions. The XPS spectrum of the 2D-hexagonal mesostructured Pt films showed two peaks at 71.0 and 74.0 eV assignable to Pt $4f_{7/2}$ and Pt $4f_{5/2}$, respectively[31] (Supporting Information, Figure S2), which indicates that Pt species are present as zerovalent.

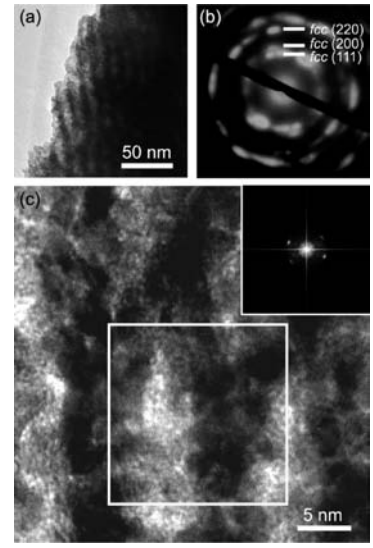

Figure 9. (a and c) TEM images and (b) ED pattern of 2D-hexagonal mesostructured Pt prepared from a precursor solution including 0.50 mL of Pt aqueous solution. Inset image of panel c is an FFT pattern of the square region of the panel. The lattice fringes of panel c correspond to Pt {111} planes due to *d*-spacings (0.23 nm) and the dihedral angle (ca. 66°). Samples for the TEM observation were scratched from the substrate and then dispersed in ethanol by ultrasound and mounted on a carbon-coated microgrid.

The cyclic voltammetry (CV) of the mesostructured Pt films showed a typical feature of the Pt electrode in aqueous H_2SO_4 solution (Figure 10). To characterize the surface of obtained mesostructured Pt films, the electrochemical method was applied because of its merit of proving the catalytic activity of surface instead of the physical surface area evaluated by the BET method of N_2 adsorption. The hydrogen adsorption and desorption were well-defined at the anodic and cathodic peaks, which are consistent with the typical CV curves of the polycrystalline nature of Pt. The CVs proved that the surfaces of these films are clean and have electrochemical activities. The removal of the block copolymers was also supported by these data. On the basis of the assumption that a monolayer of hydrogen corresponds to an adsorption charge of 210 $\mu C \cdot cm^{-2}$,[46] the electrochemically active surface areas of the mesostructured Pt films with 2D-hexagonal and cage-type were estimated to be about

(39) Lindén, M.; Schunk, S. A.; Schüth, F. *Angew. Chem., Int. Ed.* **1998**, *37*, 821.
(40) Grosso, D.; Babonneau, F.; Soler-Illia, G. J. A. A.; Albpouy, P. A.; Amenitsch, H. *Chem. Commun.* **2002**, 748.
(41) Grosso, D.; Balkenende, A. R.; Albouy, P. A.; Ayral, A.; Amenitsch, H.; Babonneau, F. *Chem. Mater.* **2001**, *13*, 1848.
(42) Yamauchi, Y.; Takai, A.; Komatsu, M.; Sawada, M.; Ohsuna, T.; Kuroda, K. *Chem. Mater.* **2008**, *20*, 1004.
(43) Luo, K.; Walker, C. T.; Edler, K. J. *Adv. Mater.* **2007**, *19*, 1506.
(44) Türker, Y.; Dag, Ö. *J. Mater. Chem.* **2008**, *18*, 3467.
(45) Kim, S. W.; Park, J.; Jang, Y.; Chung, Y.; Hwang, S.; Hyeon, T. *Nano Lett.* **2003**, *3*, 1289.
(46) Biegler, T.; Rand, D. A. J.; Woods, R. *J. Electroanal. Chem.* **1971**, *29*, 269.

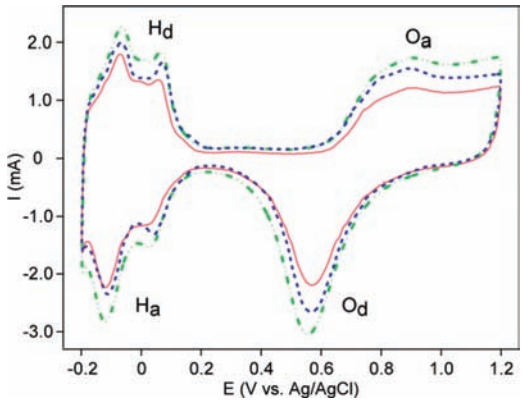

Figure 10. Cyclic voltammograms of the mesostructured Pt films in aqueous 1.0 M H_2SO_4 solution at 100 $mV \cdot s^{-1}$. Solid pink line, 2D-hexagonal; two dot chain green line, cage-type; and dashed blue line, lamellar mesostuctures. (Ha, hydrogen adsorption; Hd, hydrogen desorption; Oa, formation of Pt−O; Od, reduction of Pt oxide.)

370 $m^2 \cdot cm^{-3}$ and 430 $m^2 \cdot cm^{-3}$, respectively, from the hydrogen adsorption/desorption charge. Both values were similar to the highest values (up to 460 $m^2 \cdot cm^{-3}$) of ordered 2D-hexagonal mesoporous Pt films synthesized from $C_{16}EO_8$ on the Au electrodes.[47] The surface area expressed by the unit of $m^2 \cdot cm^{-3}$ could not be converted to the general unit of $m^2 \cdot g^{-1}$ because the density of the mesostructured Pt films could not be estimated, being due to the inhomogeneous nature of bumpy pore walls. To estimate these surface areas by the unit of $m^2 \cdot g^{-1}$, we apply a simple model of a mesoporous film (composed of Pt or SiO_2) which have perfect 2D-hexagonal mesostructures with (1) smooth mesopore surfaces, (2) no micropores, (3) uniaxial alignment (not bending), and (4) the same pore diameter and pore wall thickness as those estimated from SEM images (Figure 4). The specific surface area per volume of the assumed simple model is calculated to be about 47 $m^2 \cdot cm^{-3}$ for both Pt and SiO_2, and this value can be converted to the surface area per weight of about 2.6 $m^2 \cdot g^{-1}$ for mesoporous Pt and 25 $m^2 \cdot g^{-1}$ for mesoporous silica if the density of mesopore walls are assumed to have those of bulk Pt (21.45 $g \cdot cm^{-3}$) and amorphous silica (2.2 $g \cdot cm^{-3}$). The value of 47 $m^2 \cdot cm^{-3}$ is much lower than the experimental surface area (370 $m^2 \cdot cm^{-3}$). Therefore, the present mesostructured Pt films should contain additional surface areas due to the bumpy mesopore walls consisting of connected nanoparticles which effectively act as electrochemically active surfaces, which greatly contributes to the increase in the surface areas. Similarly, the actual surface area of the cage-type mesostructured Pt films (430 $m^2 \cdot cm^{-3}$) is much higher than the simulated surface area (94 $m^2 \cdot cm^{-3}$) of the model of cage-type of mesostructure with the same periodicity. In the case of the lamellar mesostructure, the specific surface area was about 57 cm^2 per 1 cm^2 of the film. The specific surface area per 1 cm^3 of the film was not calculated here because the film thickness was not uniform (Figure 6). From the CV measurements, the mesostructured Pt films with large periodicities have high electrochemically active surface areas, indicating that the inner parts of the films are highly accessible.

4. Conclusion

2D-Hexagonal, lamellar, and cage-type mesostructured Pt films with extralarge periodicity were successfully synthesized by changing the composition ratio of Pt species over block copolymers and by electrodeposition on Au substrates. The mesostructured films have high electrochemically active surface area due to bumpy frameworks consisting of the connected nanoparticles. The present synthetic method should be widely applicable in not only single metal systems but also binary and ternary alloy systems. The synthesis of various mesostructured metal films with extralarge periodicity opens new applications, such as electrochemical sensing and separation utilizing molecules that are too large to be treated with small mesopores.

Acknowledgment. The authors greatly appreciate the reviewers' helpful comments. The authors acknowledge Mr. M. Fuziwara (Waseda University) for TEM observation and Mr. K. Kawahara, Mr. Y. Doi, and Mr. Y. Kanno (Waseda University) for liquid-state ^1H NMR and IR measurements, respectively. The present study was supported by the Global COE Program "Practical Chemical Wisdom" from the Japanese Ministry of Education, Culture, Sports, Science, and Technology (MEXT). This work was also supported by the A3 Foresight Program "Synthesis and Structural Resolution of Novel Mesoporous Materials" and by a Grant-in-Aid for Scientific Research (No. 19850031) from the Japan Society for the Promotion of Science (JSPS). A.T. is grateful for financial support provided through a Grant-in-Aid for a JSPS Fellow from MEXT.

Supporting Information Available: XPS, IR, and liquid state ^1H NMR spectra. This material is available free of charge via the Internet at http://pubs.acs.org.

JA9062844

(47) Elliott, J. M.; Attard, G. S.; Bartlett, P. N.; Coleman, N. R. B.; Merckel, D. A. S.; Owen, J. R. *Chem. Mater.* **1999**, *11*, 3602.